

Single-Event Effects Test Report of the OPA4277-SP High-Precision Operational Amplifiers

Ram Gooty, Joel Cruz-Colon, Veeraraghavan Narayanan, Christian Yots, and Dr. Robert Baumann

ABSTRACT

The purpose of this study was to characterize the effects of heavy-ion irradiation on the single-event effect (SEE) performance of the OPA4277-SP High-Precision Operational Amplifier. Heavy-ions with an LET_{EFF} of 86 MeV-cm²/mg were used to irradiate the devices with a fluence of 1×10^7 ions/cm². The results demonstrate that the OPA4277-SP is SEL-free up to $LET_{EFF} = 86$ MeV-cm²/mg at 125°C, and dynamic SET cross section is presented.

Contents

1	Overview	2
2	SEE Mechanisms	3
3	Test Device and Test Board Information	4
4	Irradiation Facility and Setup	6
5	Results	7
6	Summary	10
Appendix A	Total Ionizing Dose From SEE Experiments	11
Appendix B	Confidence Interval Calculations	12
Appendix C	Orbital Environment Estimations	14
Appendix D	References	17

List of Figures

1	OPA4277-SP Functional Block Diagram	3
2	OPA4277-SP Temp Sensor Evaluation Module Board	4
3	Schematic of the OPA4277-SP Evaluation Board Used to Perform the SEE	5
4	Illustration of the Evaluation Board Mounted in Front of the Heavy Ion Beam Exit Port at the TAMU Accelerator Facility With a 40-mm Air Gap.....	6
5	Current vs Time (I vs t) Data for VCC Supply Current During SEL Run #26	7
6	Number of Occurrences vs Voltage (# vs V).....	8
7	Voltage Recovery vs Time (V vs μ s)	9
8	Integral Particle Flux vs LET_{EFF}	15
9	Device Cross Section vs LET_{EFF}	16

List of Tables

1	Overview Information.....	2
2	Ion Used for SEE Characterization and Effective LET_{EFF}	6
3	OPA4277-SP SEL Conditions Using ⁵⁹ Pr at an Angle-of-Incidence of 0° and 45°.....	7
4	Experimental Example Calculation of Mean-Fluence-to-Failure (MFTF) and σ Using a 95% Confidence Interval	13

Trademarks

All trademarks are the property of their respective owners.

1 Overview

The OPA4277-SP precision operational amplifier replaces the industry standard LM124-SP. It offers improved noise and two orders of magnitude lower input offset voltage. Features include ultra-low offset voltage and drift, low-bias current, high common mode rejection, and high-power supply rejection. The OPA4277-SP operates from ± 2 - to ± 18 -V supplies with excellent performance. Unlike most operational amplifiers which are specified at only one supply voltage, the OPA4277-SP precision operational amplifier is specified for real-world applications; a single limit applies over the ± 5 - to ± 15 -V supply range. High performance is maintained as the amplifier swings to the specified limits. The OPA4277-SP is easy to use and free from phase inversion and overload problems found in some operational amplifiers. It is stable in unity gain and provides excellent dynamic behavior over a wide range of load conditions. The OPA4277-SP features completely independent circuitry for lowest crosstalk and freedom from interaction, even when overdriven or overloaded.

www.ti.com/product/OPA4277-SP/technicaldocuments.

Table 1. Overview Information⁽¹⁾

TI Part Number	OPA4277-SP
SMD Number	5962L1620901VXA
Device Function	Remote and Local Digital Temperature Sensor
Technology	BIPOLAR
Exposure Facility	Radiation Effects Facility, Cyclotron Institute, Texas A&M University
Heavy Ion Fluence per Run	1×10^6 – 1×10^7 ions/cm ²
Irradiation Temperature	25°C and 125°C (for SEL testing)

⁽¹⁾ TI may provide technical, applications or design advice, quality characterization, and reliability data or service providing these items shall not expand or otherwise affect TI's warranties as set forth in the Texas Instruments Incorporated Standard Terms and Conditions of Sale for Semiconductor Products and no obligation or liability shall arise from Semiconductor Products and no obligation or liability shall arise from TI's provision of such items.

2 SEE Mechanisms

The primary single-event effect (SEE) events of interest in the OPA4277-SP are single-event latch-up (SEL), single-event burn-out (SEB) and single-event transient (SET). From a risk/impact point-of-view, the occurrence of an SEL and SEB is potentially the most destructive SEE event and the biggest concern for space applications. In mixed technologies such as the BIPOLAR process used for the OPA4277-SP, the CMOS circuitry introduces a potential for SEL and SEB susceptibility. SEL can occur if excess current injection caused by the passage of an energetic ion is high enough to trigger the formation of a parasitic cross-coupled PNP and NPN bipolar structure (formed between the p-sub and n-well and n+ and p+ contacts). The parasitic bipolar structure initiated by a single-event creates a high-conductance path (inducing a steady-state current that is typically orders-of-magnitude higher than the normal operating current) between power and ground that persists (is “latched”) until power is removed or until the device is destroyed by the high-current state. The process modifications applied for SEL-mitigation were sufficient as the OPA4277-SP exhibited no SEL with heavy-ions up to an LET_{EFF} of 86 MeV-cm²/mg at a fluence of 10⁷ ions/cm² and a chip temperature of 125°C.

Study was performed to evaluate the cross section and transient effects with an inverting gain configuration. The input was grounded and gain was set to 10 V/V to provide maximum voltage swing during upsets. To capture different SET signatures events device rails were set to max levels of ±7 V for output load condition of 600 Ω. Further data points were taken at max supply rail of ±15 V under various loads of 1k, 2k and 10k to evaluate difference in upset rate with load and rail voltages. The output voltage was monitored for the transients during the beam exposure. Heavy ions with LET_{EFF} 10, 21, 30, 60 and 85 MeV-cm²/mg were used to irradiate the devices. Flux of 10⁵ ions/s-cm² and fluence of 10⁷ ions/cm² were used during the exposure at room temp. The output transient data was processed and analyzed for the following criteria:

1. Transient height or level.
2. Transient time taken to get back to set level on output.

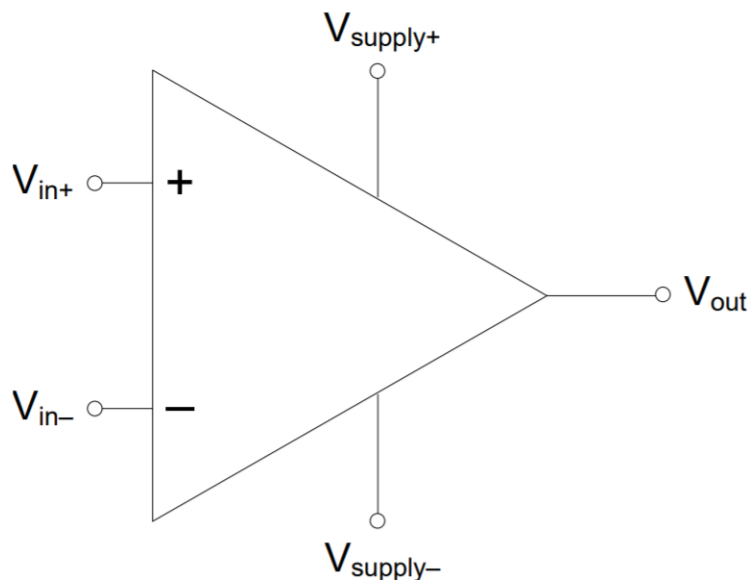


Figure 1. OPA4277-SP Functional Block Diagram

3 Test Device and Test Board Information

The OPA4277-SP has 14 pad and released in KGD package for SEL/SET testing purpose the device is packaged in a 24-pin, CDIP package with 14 pads bonded out. The OPA4277-SP evaluation board is an in-house built 2 Layer PCB. The board was powered up with two voltage rails using two of the four channels of the Agilent N6702A precision power supply and loaded with a discrete 600-Ω resistor. Evaluation board used for the SEE characterization is shown in [Figure 2](#) and schematics are presented in [Figure 3](#).

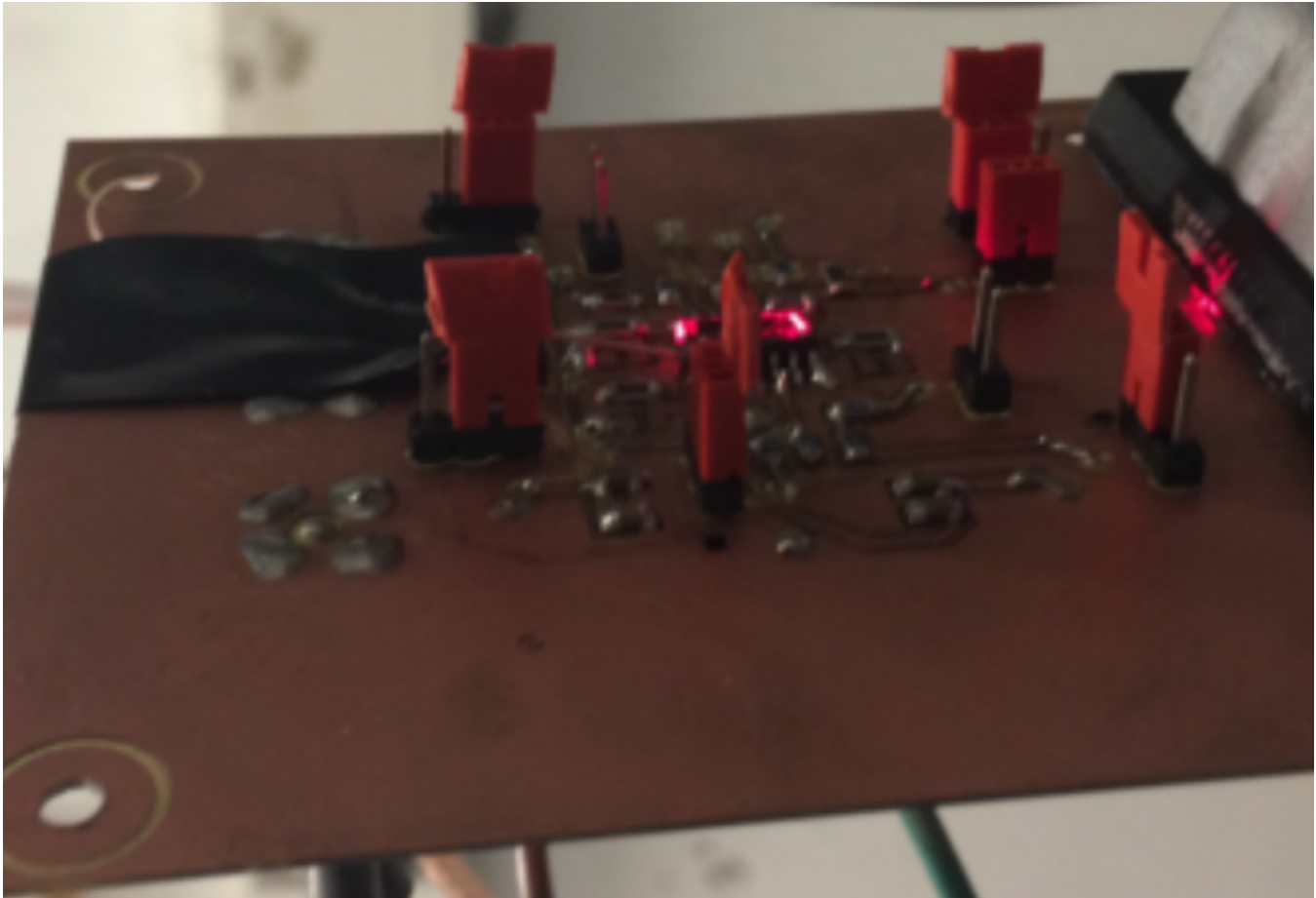


Figure 2. OPA4277-SP Temp Sensor Evaluation Module Board

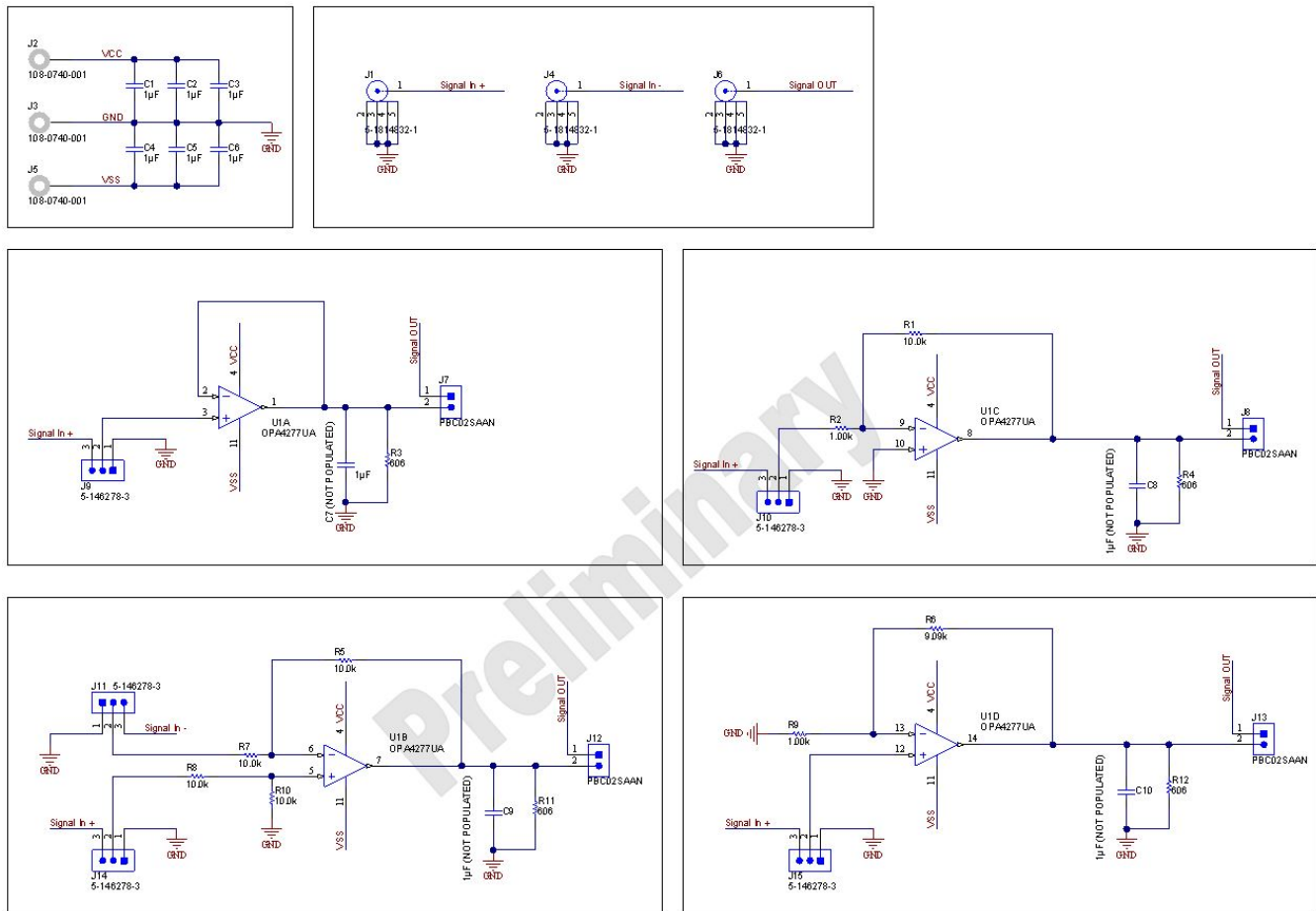


Figure 3. Schematic of the OPA4277-SP Evaluation Board Used to Perform the SEE

4 Irradiation Facility and Setup

The heavy ion species used for the SEE studies on this product were provided and delivered by the TAMU Cyclotron Radiation Effects Facility[3] using a superconducting cyclotron and advanced electron cyclotron resonance (ECR) ion source. Ion beams are delivered with high uniformity over a 1-in diameter circular cross sectional area for the in-air station. Uniformity is achieved by means of magnetic defocusing. The intensity of the beam is regulated over a broad range spanning several orders of magnitude. For the bulk of these studies, ion fluxes between 10^4 and 10^5 ions/s-cm² were used to provide heavy ion fluences between 10^6 and 10^7 ions/cm². For these experiments, Neon (Ne), Argon (Ar), Copper (Cu), Silver (Ag) and Praseodymium (Pr), ions were used. Ion beam uniformity for all tests was in the range of 91% to 98%. [Figure 4](#) shows the way test boards are used for exposure at TAMU facility. The 1-mil Aramica® window allows in-air testing while maintaining the vacuum within the accelerator with only minor ion energy loss. The air space between the device and the ion beam port window was maintained at 40 mm for all runs. For more information on the effective LET, range and depth for the experiments, please refer to [Table 2](#).

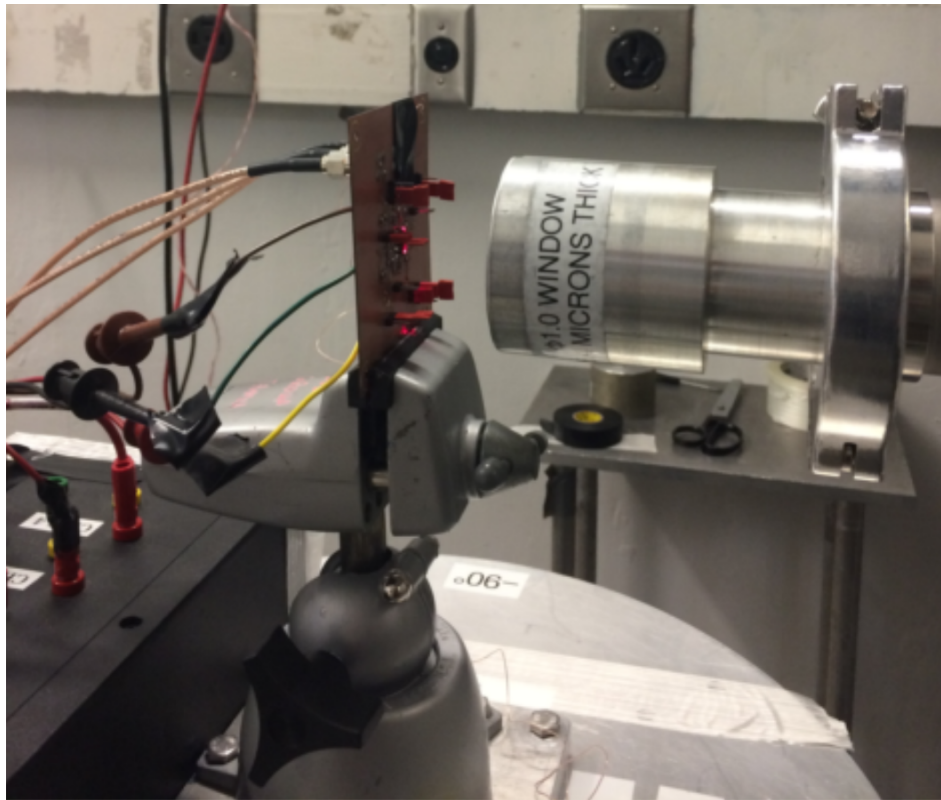


Figure 4. Illustration of the Evaluation Board Mounted in Front of the Heavy Ion Beam Exit Port at the TAMU Accelerator Facility With a 40-mm Air Gap

Table 2. Ion Used for SEE Characterization and Effective LET_{EFF}

ION TYPE	ANGLE OF INCIDENCE	FLUX (ions-cm ² /mg)	FLUENCE (# ions)	LET _{EFF} (MeV-cm ² /mg)
Ne	0	1.00E+05	1.00E+07	3
Ar	0	1.00E+05	1.00E+07	10
Cu	0	1.00E+05	1.00E+07	21
Cu	45	1.00E+05	1.00E+07	30
Ag	0	1.00E+05	1.00E+07	43
Ag	45	1.00E+05	1.00E+07	61
Pr	0	1.00E+05	1.00E+07	61
Pr	45	1.00E+05	1.00E+07	85

5 Results

5.1 Single Event Latch-Up (SEL)

During SEL characterization, the device was heated using forced hot air, maintaining the die temperature at 125°C. The temperature was monitored by means of a K-type thermocouple attached as close as possible to the die. The species used for the SEL testing was a praseodymium (⁵⁹Pr) ion with an angle-of-incidence of 0° and 45° for an LET_{EFF} = 60 and 85 MeV-cm²/mg. The kinetic energy in the vacuum for this ion is 0.885 GeV (15-MeV/amu line). A flux of approximately 10⁵ ions/cm²-s and a fluence of approximately 10⁷ ions were used for all runs. The supply voltage was set to a max value of ±15 V with the device configured in an inverting Amp configuration with a gain of 10 V/V, inputs grounded, and the supply currents were continuously monitored for latch-up. Run duration to achieve this fluence was approximately two minutes. No SEL events were observed during all four runs shown in Table 3. Figure 5 shows a plot of the current vs time.

Table 3. OPA4277-SP SEL Conditions Using ⁵⁹Pr at an Angle-of-Incidence of 0° and 45°

RUN #	DISTANCE (mm)	TEMP (°C)	ION	ANGLE (°)	FLUX (ions-cm ² /mg)	FLUENCE (# ions)	LET _{EFF} (MeV-cm ² /mg)	NOTES
26	40	125	Pr	45	1.00E+05	1.00E+07	85	No LUP
27	40	125	Pr	45	1.00E+05	1.00E+07	85	No LUP
24	40	125	Pr	0	1.00E+05	1.00E+07	65.65	No LUP
25	40	125	Pr	0	1.00E+05	1.00E+07	65.65	No LUP

No SEL events were observed, indicating that the OPA4277-SP is SEL-immune at LET_{EFF} = 85 MeV-cm²/mg and T = 125°C. Using the MFTF method described in Appendix B and combining (or summing) the fluences of the runs (4 × 10⁷), the upper-bound cross-section (using a 95% confidence level) is calculated as:

$$\sigma_{SEL} \leq 2.65 \times 10^{-7} \text{ cm}^2 \text{ for } LET_{EFF} = 85 \text{ MeV-cm}^2/\text{mg} \text{ and } T = 125^\circ\text{C} \quad (1)$$

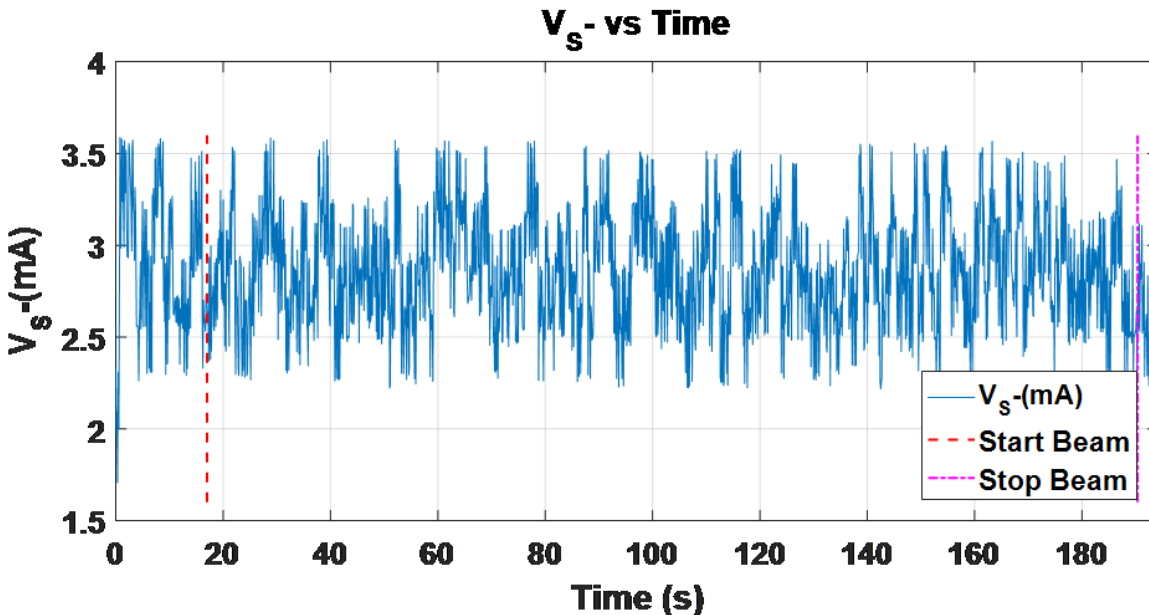


Figure 5. Current vs Time (I vs t) Data for VCC Supply Current During SEL Run #26

5.2 SET

Study was performed to evaluate the cross section and transient effects on an inverting gain configuration. The Input was grounded and gain was set to 10 V/V to provide maximum voltage swing during upsets. Device rails were set to max levels of ± 7 V for output load condition of 600 Ω . Further data points were taken at max supply rail of ± 15 V under various loads of 1k, 2k, and 10k to evaluate difference in upset rate with load and rail voltages. The output voltage was monitored for the transients during the beam exposure. Heavy Ions with LET_{EFF} of 10, 21, 30, 60 and 85 MeV-cm²/mg were used to irradiate the devices. Flux of 10⁴ ions/s-cm² and fluence of 10⁶ ions/cm² were used during the exposure. The output transient data was processed and analyzed to study the following two criteria:

1. **Transient height or level:** a typical histogram of the transient height analysis at LET_{EFF} of 85 MeV and 10k load with a voltage rail of ± 15 V is displayed below. Majority of events fall below 1 V and there are some large events seen but none seen going up to rail voltage across various runs. [Figure 6](#) shows the histogram plot for number of occurrences vs voltage.

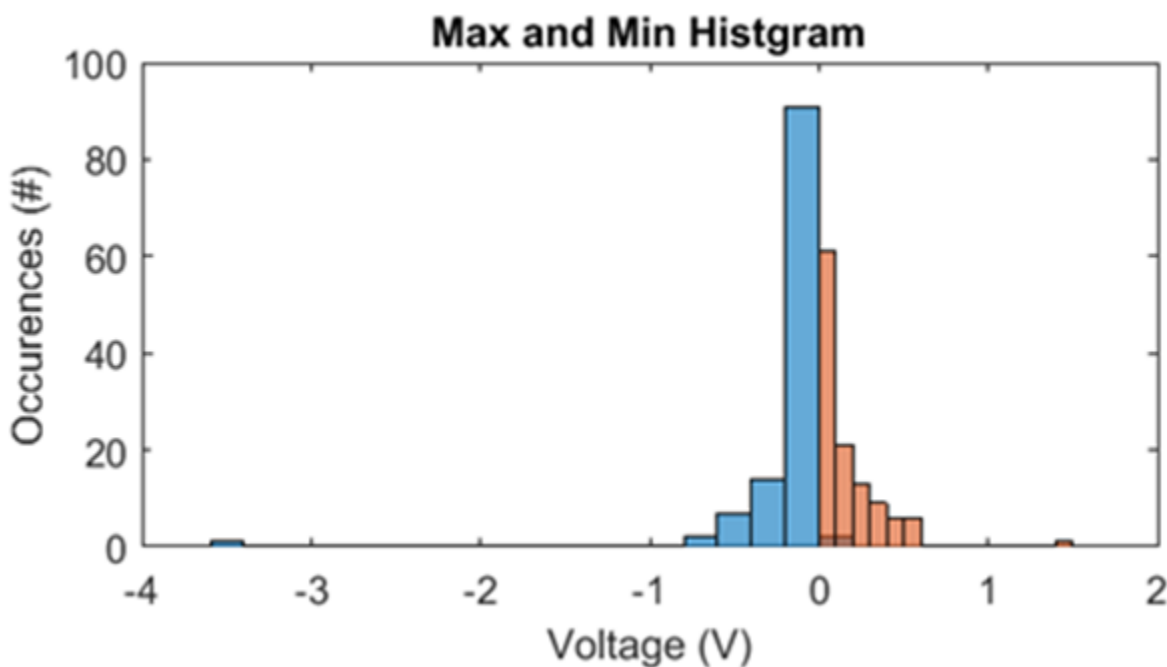


Figure 6. Number of Occurrences vs Voltage (# vs V)

2. **Transient time taken to get back to set level on output:** A typical overlay plot of all events at LET_{EFF} of 85 MeV and 10k load with a voltage rail of ± 15 V is displayed below. Most of the events are in micro second range with max < 10 μ s. This small recovery time is also key from an application stand point since integration techniques can be applied very easily on data to avoid any influence to the signal data. [Figure 7](#) shows the scatter plot of voltage recovery vs time.

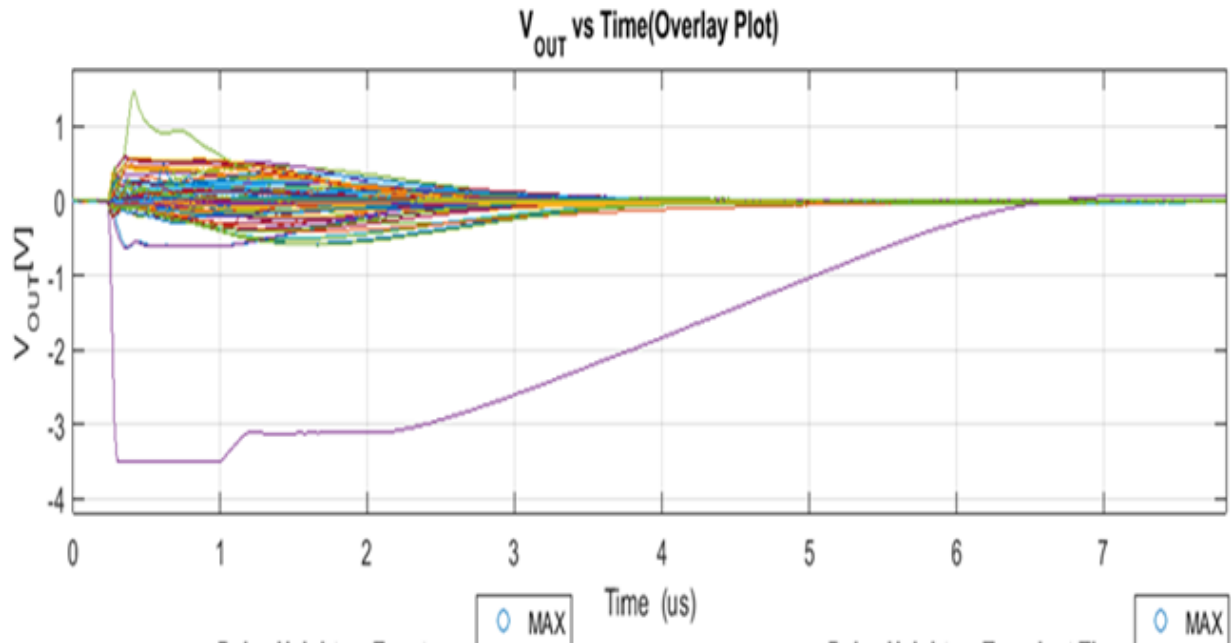


Figure 7. Voltage Recovery vs Time (V vs μs)

$$\sigma = \frac{\chi^2(d+1)100(1-\frac{\alpha}{2})}{2nF} \tag{2}$$

$$\sigma_{SEL} \leq 3.09 \times 10^{-3} \text{ cm}^2 \text{ for } LET_{EFF} = 85 \text{ MeV-cm}^2/\text{mg} \text{ and } T=25^\circ\text{C} @ 10\text{KOhm load} \tag{3}$$

6 Summary

Radiation effects of High Precision Operational Amplifier OPA4277-SP was studied. This device pass total dose rate of up to 50 krad(Si) and is latch-up immune up to 85 MeV. Single event transient study was done showing the various type of transients possible. Most of the transients were in the microseconds range and below 1 V. Based on the transient timing, these events should be easily mitigated by integration techniques in application. There were no transients observed up to rail voltage which is a key concern.

Total Ionizing Dose From SEE Experiments

The production OPA4277-SP High Precision Operational Amplifier rated for operation to a total ionizing dose (TID) of 50 krad(Si). In the course of the SEE testing, the heavy-ion exposures delivered a little bit less than ~1 krad(Si) per 10^6 ions/cm² run.

Confidence Interval Calculations

For conventional products where hundreds of failures are seen during a single exposure, one can determine the average failure rate of parts being tested in a heavy-ion beam as a function of fluence with high degree of certainty and reasonably tight standard deviation, and thus have a good deal of confidence that the calculated cross-section is accurate.

With radiation hardened parts however, determining the cross-section becomes more difficult since often few, or even, no failures are observed during an entire exposure. Determining the cross-section using an average failure rate with standard deviation is no longer a viable option, and the common practice of assuming a single error occurred at the conclusion of a null-result can end up in a greatly underestimated cross-section.

In cases where observed failures are rare or non-existent, the use of confidence intervals and the chi-squared distribution is indicated. The Chi-Squared distribution is particularly well-suited for the determination of a reliability level when the failures occur at a constant rate. In the case of SEE testing, where the ion events are random in time and position within the irradiation area, one expects a failure rate that is independent of time (presuming that parametric shifts induced by the total ionizing dose do not affect the failure rate), and thus the use of chi-squared statistical techniques is valid (since events are rare an exponential or Poisson distribution is usually used).

In a typical SEE experiment, the device-under-test (DUT) is exposed to a known, fixed fluence (ions/cm²) while the DUT is monitored for failures. This is analogous to fixed-time reliability testing and, more specifically, time-terminated testing, where the reliability test is terminated after a fixed amount of time whether or not a failure has occurred (in the case of SEE tests fluence is substituted for time and hence it is a fixed fluence test) [5]. Calculating a confidence interval specifically provides a range of values which is likely to contain the parameter of interest (the actual number of failures/fluence). Confidence intervals are constructed at a specific confidence level. For example, a 95% confidence level implies that if a given number of units were sampled numerous times and a confidence interval estimated for each test, the resulting set of confidence intervals would bracket the true population parameter in about 95% of the cases.

In order to estimate the cross-section from a null-result (no fails observed for a given fluence) with a confidence interval, we start with the standard reliability determination of lower-bound (minimum) mean-time-to-failure for fixed-time testing (an exponential distribution is assumed):

$$MTTF = \frac{2nT}{\chi^2_{2(d+1); 100\left(1-\frac{\alpha}{2}\right)}} \tag{4}$$

Where *MTTF* is the minimum (lower-bound) mean-time-to-failure, *n* is the number of units tested (presuming each unit is tested under identical conditions) and *T*, is the test time, and χ^2 is the chi-square distribution evaluated at $100(1 - \alpha / 2)$ confidence level and where *d* is the degrees-of-freedom (the number of failures observed). With slight modification for our purposes we invert the inequality and substitute *F* (fluence) in the place of *T*:

$$MFTF = \frac{2nF}{\chi^2_{2(d+1); 100\left(1-\frac{\alpha}{2}\right)}} \tag{5}$$

Where now *MFTF* is mean-fluence-to-failure and *F* is the test fluence, and as before, χ^2 is the chi-square distribution evaluated at $100(1 - \alpha / 2)$ confidence and where *d* is the degrees-of-freedom (the number of failures observed). The inverse relation between MTTF and failure rate is mirrored with the MFTF. Thus the upper-bound cross section is obtained by inverting the MFTF:

$$\sigma = \frac{\chi^2_{2(d+1); 100\left(1-\frac{\alpha}{2}\right)}}{2nF} \quad (6)$$

Let's assume that all tests are terminated at a total fluence of 10^6 ions/cm². Let's also assume that we have a number of devices with very different performances that are tested under identical conditions. Assume a 95% confidence level ($\sigma = 0.05$). Note that as d increases from 0 events to 100 events the actual confidence interval becomes smaller, indicating that the range of values of the true value of the population parameter (in this case the cross section) is approaching the mean value + 1 standard deviation. This makes sense when one considers that as more events are observed the statistics are improved such that uncertainty in the actual device performance is reduced.

Table 4. Experimental Example Calculation of Mean-Fluence-to-Failure (MFTF) and σ Using a 95% Confidence Interval⁽¹⁾

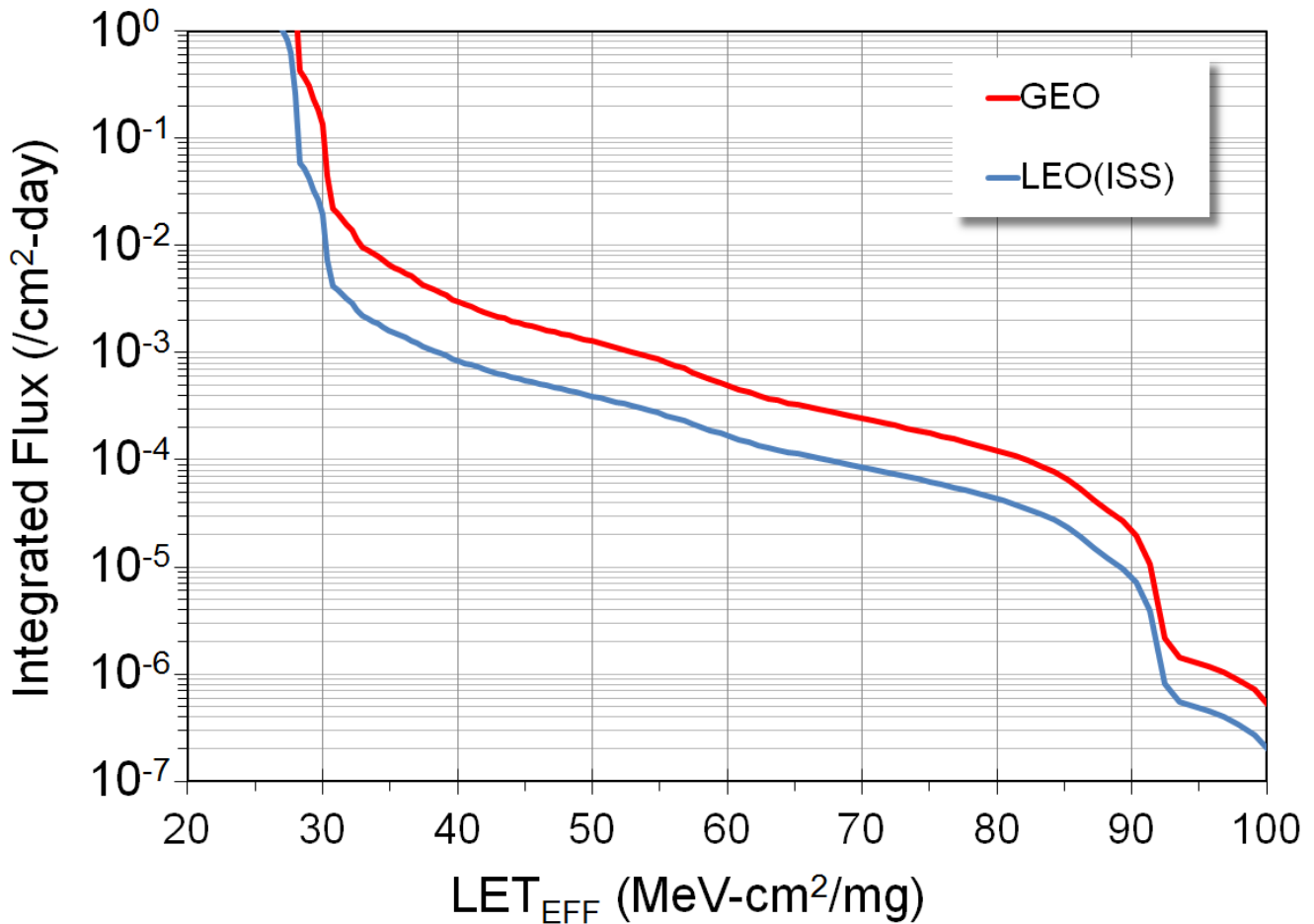
Degrees-of-Freedom (d)	2(d + 1)	χ^2 @ 95%	Calculated Cross Section (cm ²)		
			Upper-Bound @ 95% Confidence	Mean	Average + Standard Deviation
0	2	7.38	3.69E-06	0.00E+00	0.00E+00
1	4	11.14	5.57E-06	1.00E-06	2.00E-06
2	6	14.45	7.22E-06	2.00E-06	3.41E-06
3	8	17.53	8.77E-06	3.00E-06	4.73E-06
4	10	20.48	1.02E-05	4.00E-06	6.00E-06
5	12	23.34	1.17E-05	5.00E-06	7.24E-06
10	22	36.78	1.84E-05	1.00E-05	1.32E-05
50	102	131.84	6.59E-05	5.00E-05	5.71E-05
100	202	243.25	1.22E-04	1.00E-04	1.10E-04

⁽¹⁾ Using a 95% confidence for several different observed results (d = 0, 1, 2, and 3 observed events during fixed-fluence tests) on four identical devices and test conditions.

Orbital Environment Estimations

In order to calculate on-orbit SEE event rates one needs both the device SEE cross-section and the flux of particles encountered in a particular orbit. Device SEE cross-sections are usually determined experimentally while flux of particles in orbit is calculated using various codes. For the purpose of generating some event rates, a Low-Earth Orbit (LEO) and a Geostationary-Earth Orbit (GEO) were calculated using CREME96. CREME96 code, short for Cosmic Ray Effects on Micro-Electronics is a suite of programs [6][7] that enable estimation of the radiation environment in near-Earth orbits. CREME96 is one several tools available in the aerospace industry to provide accurate space environment calculations. Over the years since its introduction, the CREME models have been compared with on-orbit data and demonstrated their accuracy. In particular, CREME96 incorporates realistic “worst-case” solar particle event models, where fluxes can increase by several orders-of-magnitude over short periods of time.

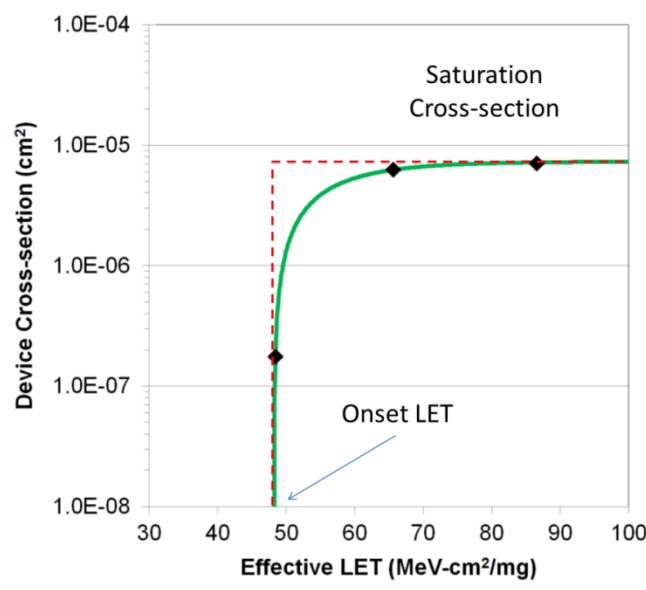
For the purposes of generating conservative event rates, the worst-week model (based on the biggest solar event lasting a week in the last 45 years) was selected, which has been equated to a 99%-confidence level worst-case event [8][9]. The integrated flux includes protons to heavy ions from solar and galactic sources. A minimal shielding configuration is assumed at 100 mils (2.54 mm) of aluminum. Two orbital environments were estimated, that of the International Space Station (ISS) which is LEO and the GEO environment. [Figure 8](#) shows the integrated flux (from high LET to low) for these two environments.



NOTE: LEO(ISS) (blue) and a GEO (red) environment as calculated by CREME96 assuming worst-week and 100 mils (2.54 mm) of aluminum shielding.

Figure 8. Integral Particle Flux vs LET_{EFF}

Using this data, we can extract integral particle fluxes for any arbitrary LET of interest. To simplify the calculation of event rates we assume that all cross-section curves are square – meaning that below the onset LET the cross-section is identically zero while above the onset LET the cross-section is uniformly equal to the saturation cross-section. Figure 9 illustrates the approximation, with the green curve being the actual Weibull fit to the data with the “square” approximation shown as the red-dashed line. This allows us to calculate event rates with a single multiplication, the event rate becoming simply the product of the integral flux at the onset LET, and the saturation cross-section. Obviously this leads to an over-estimation of the event rate since the area under the square approximation is larger than the actual cross-section curve – but for the purposes of calculating upper-bound event rate estimates, this modification avoids the need to do the integral over the flux and cross-section curves.



(1) Weibull Fit (green) is "simplified" with the use of a square approximation (red dashed line).

Figure 9. Device Cross Section vs LET_{EFF}

To demonstrate how the event rates in this report were calculated, assume that we wish to calculate an event rate for a GEO orbit for the device whose cross-section is shown in Figure 9. Using the red curve in Figure 9 and the onset LET value obtained from the Figure 8 (~ 47 MeV-cm²/mg) we find the GEO integral flux to be ~ 1.6 × 10⁻³ ions/cm²-day. The event rate is the product of the integral flux and the saturation cross-section in Figure 9 (~ 7.5 × 10⁻⁶ cm²):

$$GEO \text{ Event Rate} = (1.6 \times 10^{-3} \frac{\text{ions}}{\text{cm}^2 \times \text{day}}) \times (7.5 \times 10^{-6} \text{cm}^2) = 1.2 \times 10^{-8} \frac{\text{events}}{\text{day}}$$

$$GEO \text{ Event Rate} = 5.0 \times 10^{-10} \frac{\text{events}}{\text{hr}} = 0.5 \text{ FIT}$$

$$MTBE = 234,000 \text{ Years!}$$

(7)

References

1. M. Shoga and D. Binder, “Theory of Single Event Latchup in Complementary Metal-Oxide Semiconductor Integrated Circuits”, IEEE Trans. Nucl. Sci, Vol. 33(6), Dec. 1986, pp. 1714-1717.
2. G. Bruguier and J.M. Palau, “Single particle-induced latchup”, IEEE Trans. Nucl. Sci, Vol. 43(2), Mar. 1996, pp. 522-532.
3. TAMU Radiation Effects Facility website. <http://cyclotron.tamu.edu/ref/>
4. “The Stopping and Range of Ions in Matter” (SRIM) software simulation tools website. <http://www.srim.org/index.htm#SRIMMENU>
5. D. Kececioglu, “Reliability and Life Testing Handbook”, Vol. 1, PTR Prentice Hall, New Jersey, 1993, pp. 186-193.
6. <https://creme.isde.vanderbilt.edu/CREME-MC>
7. A. J. Tylka, et al., “CREME96: A Revision of the Cosmic Ray Effects on Micro-Electronics Code”, IEEE Trans. Nucl. Sci., 44(6), 1997, pp. 2150-2160.
8. A. J. Tylka, W. F. Dietrich, and P. R. Bobery, “Probability distributions of high-energy solar-heavy-ion fluxes from IMP-8: 1973-1996”, IEEE Trans. on Nucl. Sci., 44(6), Dec. 1997, pp. 2140 – 2149.
9. A. J. Tylka, J. H. Adams, P. R. Boberg, et al., “CREME96: A Revision of the Cosmic Ray Effects on Micro-Electronics Code”, Trans. on Nucl. Sci, 44(6), Dec. 1997, pp. 2150 – 2160.

IMPORTANT NOTICE FOR TI DESIGN INFORMATION AND RESOURCES

Texas Instruments Incorporated ("TI") technical, application or other design advice, services or information, including, but not limited to, reference designs and materials relating to evaluation modules, (collectively, "TI Resources") are intended to assist designers who are developing applications that incorporate TI products; by downloading, accessing or using any particular TI Resource in any way, you (individually or, if you are acting on behalf of a company, your company) agree to use it solely for this purpose and subject to the terms of this Notice.

TI's provision of TI Resources does not expand or otherwise alter TI's applicable published warranties or warranty disclaimers for TI products, and no additional obligations or liabilities arise from TI providing such TI Resources. TI reserves the right to make corrections, enhancements, improvements and other changes to its TI Resources.

You understand and agree that you remain responsible for using your independent analysis, evaluation and judgment in designing your applications and that you have full and exclusive responsibility to assure the safety of your applications and compliance of your applications (and of all TI products used in or for your applications) with all applicable regulations, laws and other applicable requirements. You represent that, with respect to your applications, you have all the necessary expertise to create and implement safeguards that (1) anticipate dangerous consequences of failures, (2) monitor failures and their consequences, and (3) lessen the likelihood of failures that might cause harm and take appropriate actions. You agree that prior to using or distributing any applications that include TI products, you will thoroughly test such applications and the functionality of such TI products as used in such applications. TI has not conducted any testing other than that specifically described in the published documentation for a particular TI Resource.

You are authorized to use, copy and modify any individual TI Resource only in connection with the development of applications that include the TI product(s) identified in such TI Resource. NO OTHER LICENSE, EXPRESS OR IMPLIED, BY ESTOPPEL OR OTHERWISE TO ANY OTHER TI INTELLECTUAL PROPERTY RIGHT, AND NO LICENSE TO ANY TECHNOLOGY OR INTELLECTUAL PROPERTY RIGHT OF TI OR ANY THIRD PARTY IS GRANTED HEREIN, including but not limited to any patent right, copyright, mask work right, or other intellectual property right relating to any combination, machine, or process in which TI products or services are used. Information regarding or referencing third-party products or services does not constitute a license to use such products or services, or a warranty or endorsement thereof. Use of TI Resources may require a license from a third party under the patents or other intellectual property of the third party, or a license from TI under the patents or other intellectual property of TI.

TI RESOURCES ARE PROVIDED "AS IS" AND WITH ALL FAULTS. TI DISCLAIMS ALL OTHER WARRANTIES OR REPRESENTATIONS, EXPRESS OR IMPLIED, REGARDING TI RESOURCES OR USE THEREOF, INCLUDING BUT NOT LIMITED TO ACCURACY OR COMPLETENESS, TITLE, ANY EPIDEMIC FAILURE WARRANTY AND ANY IMPLIED WARRANTIES OF MERCHANTABILITY, FITNESS FOR A PARTICULAR PURPOSE, AND NON-INFRINGEMENT OF ANY THIRD PARTY INTELLECTUAL PROPERTY RIGHTS.

TI SHALL NOT BE LIABLE FOR AND SHALL NOT DEFEND OR INDEMNIFY YOU AGAINST ANY CLAIM, INCLUDING BUT NOT LIMITED TO ANY INFRINGEMENT CLAIM THAT RELATES TO OR IS BASED ON ANY COMBINATION OF PRODUCTS EVEN IF DESCRIBED IN TI RESOURCES OR OTHERWISE. IN NO EVENT SHALL TI BE LIABLE FOR ANY ACTUAL, DIRECT, SPECIAL, COLLATERAL, INDIRECT, PUNITIVE, INCIDENTAL, CONSEQUENTIAL OR EXEMPLARY DAMAGES IN CONNECTION WITH OR ARISING OUT OF TI RESOURCES OR USE THEREOF, AND REGARDLESS OF WHETHER TI HAS BEEN ADVISED OF THE POSSIBILITY OF SUCH DAMAGES.

You agree to fully indemnify TI and its representatives against any damages, costs, losses, and/or liabilities arising out of your non-compliance with the terms and provisions of this Notice.

This Notice applies to TI Resources. Additional terms apply to the use and purchase of certain types of materials, TI products and services. These include; without limitation, TI's standard terms for semiconductor products (<http://www.ti.com/sc/docs/stdterms.htm>), [evaluation modules](#), and [samples](http://www.ti.com/sc/docs/sampterm.htm) (<http://www.ti.com/sc/docs/sampterm.htm>).

Mailing Address: Texas Instruments, Post Office Box 655303, Dallas, Texas 75265
Copyright © 2018, Texas Instruments Incorporated